Two-gluon model of hadronic transitions between S, D, and P states in $c\bar{c}$ and $b\bar{b}$ systems

M. Chemtob and H. Navelet
Service de Physique Théorique CEN-Saclay 91191 Gif-sur-Yvette CEDEX, France
(Received 10 November 1989)

The hadronic transitions between the narrow excited states of orbital angular momentum S, D, and P in the charmonium and bottomonium systems are described as two-gluon emission processes and their probability amplitudes evaluated in the semiperturbative approach based on Feynman diagrams. The hadronization amplitudes of gluons into the light hadrons are introduced by projecting onto the states of zero intrinsic angular momentum of the two gluons. The transition rates into the two space-parity channels $0^{\pm}$ are considered. Detailed predictions are presented for the rates and mass distributions in the $\pi\pi$ and η,π^0 channels. The matching of theory with data necessitates the incorporation of a large enhancement factor in the 0^- channel relative to the 0^+ channel, for which one possible interpretation is that the color coupling constant for magnetic gluons exceeds significantly that for electric gluons. We compare our results to those of the QCD multipole-expansion approach.

I. INTRODUCTION

Since the first experimental observation around 1975 of the hadronic cascade transitions within the J/ψ system,[1] $\psi' \to \psi + h$, a large body of experimental data has been accumulated (see[2] for a list of references). Measurements are available today for integrated as well as differential transition rates with respect to mass and angles of the emitted light hadrons ($h = \pi\pi, \eta, \pi^0$), both for the $c\bar{c}$ and $b\bar{b}$ systems and in a variety of initial- and final-state configurations $S \to S$, $D \to S$, and $P \to S$. More data are due to come in the future from the e^-e^+ and $p\bar{p}$ colliders, since, besides their intrinsic interest, hadronic transitions have an important use in tagging the quarkonia excited states.

Based on the Okubo-Zweig-Iizuka (OZI) rule, it has been customary to associate the observed small metastability of the narrow states, which lie below or close to the heavy-flavor energy threshold, with respect to decay to the lower-energy states as a two-step process $(Q\bar{Q}) \to (Q\bar{Q}) + gg \to (Q\bar{Q}) + h$ in which the heavy-quark system initially emits two or more gluons which subsequently hadronize into light hadrons. From this point of view, the phenomenology of the hadronic cascade transitions should, among other things, constitute a potentially valuable source of information on soft multigluon systems in the interval of invariant masses 0–1000 MeV.

The hadronic cascade transitions were initially discussed within the current-algebra framework.[3] Next came QCD-inspired calculations which were based on a Feynman-diagram description of the two-gluon emission amplitude.[4,5] However, the constituent quark-gluon approach was soon abandoned by most researchers in favor of the QCD approach based on the multipole and short-distance expansions.[6–8] While the comparison of both the Feynman graph and QCD multipole approaches with experiment gives clear indications that the picture based on the OZI rule is basically sound, the intrusion of nonperturbative physics has caused the theoretical understanding of this branch of heavy-quark phenomenology to remain to this day largely semiquantitative. Discrepancies between the two approaches, between the various multipole models and between theory and experiment attain in certain cases 1 to 2 orders of magnitudes.

In spite of its attractiveness in separating out the nonperturbative structure effects at the heavy-quark vertex part and in incorporating the low-energy theorem constraints at the light-quark vertex part,[9–12] the multipole approach is not beyond critique. First, its applicability rests on the low-energy approximation $ka \lesssim 1$ where k is a typical gluon momentum and a a typical linear size parameter for the $Q\bar{Q}$ system. For the two-gluon emission case, $k \simeq \frac{1}{2}(\Delta^2 - W^2)^{1/2}$ where W is the invariant mass and $\Delta = M_b - M_a$ is the maximum available transition energy. Combining the choice $\Delta = 500$ MeV with typical potential-model estimates of the size, $a \simeq 0.5-1.0$ fm (charmonium), $a \simeq 0.2-0.7$ fm (bottomonium), we find that ka varies from 0.5 to 1.25 (charmonium) and from 0.2 to 0.5 (bottomonium). Note now that most of the existing transitions have $\Delta = 500-1000$ MeV, corresponding to a doubling of ka. Thus, one sees that the long-wavelength approximation could be easily invalidated for energetic gluons and/or for the large-size excited states lying close to the threshold for opening of the new flavor.

The multipole approach also requires for its practical implementation an assumption on the color excited states of the heavy quarks on which there exists no experimental control. Thus the low-energy framework of Voloshin and Zakharov[9,11] and Novikov and Shifman[10] (VZNS) relies on a local approximation for the heavy-quark propagation kernel which is strictly valid in the limit of infinitely massive quarks. In fact, the systematic comparison with experiment of absolute predictions for the various transition rates[12] obtained with the local approximation results in a situation which is not very satisfactory. Also for the interesting η-meson production case,[9] in order to apply the low-energy theorem which follows from the axial-vector-current anomaly, one must discard on the basis of rather weak justifications certain operators involving the gluon fields.

The local approximation can, of course, be avoided, but at the cost of introducing a specific model to describe the intermediate states of the heavy quarks in the presence of gluons. Kuang and Yan[13] have discussed two interesting applications of the multipole-expansion approach not subject to the local approximation: a vibrating-string model for the color-octet $\bar{Q}Q$ states and a partonic two-gluon model. The various versions of their models yield results[13,14] which miss or overshoot those of the soft-pion model of Voloshin and Zakharov by one or more orders of magnitudes depending on the transition type.

Summarizing the above we see that apart from the possibility that the multipole approach may not be quantitatively reliable for the heavy-quark systems of interest, it faces us with the dilemma of choosing between an inaccurate low-energy local approximation and a hybrid model for the structure of the heavy-quark systems. It should also be mentioned here that the predictive power of the multipole approach is somewhat limited, since for each new configuration of the initial and final bound states one must associate new adjustable constant parameters to the various matrix elements. Finally, measurements[2] of the $\Upsilon(3S)$ hadronic decay rates, which became available in the past few years, have revealed an unexpected flattening of the $\pi\pi$ invariant-mass spectrum at the low W end of the spectrum (collinear pions), which have defied so far all the simple explanations within the multipole approach. It has been shown recently that the origin of the observed low W enhancements does not reside either in the retardation effects nor in a $\pi\pi$ final-state interaction.[15] The explanation, due originally to Voloshin,[15] in terms of a $\Upsilon\pi$ four-quark resonance remains a possibility.[15] An alternative plausible explanation could arise in a quark-gluon approach via a mechanism where the two pions are emitted sequentially,[16] corresponding to an enhanced s-channel contribution $\pi+\Upsilon''\to\pi+\Upsilon$.

The above observations have motivated us to return to the past history of the hadronic cascade transitions in an attempt to reexamine an application of the quark-gluon approach initiated some time ago by Billoire, Lacaze, Morel, and Navelet[5] (BLMN). Even though this approach rests on a weaker theoretical basis than the multipole approach, it may still provide some useful physical insights. In a few words, this is a semiperturbative Feynman-diagram description where the quarks and gluons are treated as constituent partons. A crucial element to the success of this approach lies in the use of a hadronization prescription which consists of a projection on the zero value of the intrinsic angular momentum of the two-gluon system, with no restrictions on the orbital momentum of the gluon pair relative to the heavy quarks.

In the present work, we shall pursue the phenomenological analysis of BLMN by calculating the transition amplitudes for both angular momentum and parity $0^{\pm}$ channels of the light mesons in the various S-, D-, and P-state configurations of the initial and final states of the heavy-quark system where measurements are either available or due. Recognizing the relevance of the relativistic and of the off-mass-shell effects, we shall first discuss the construction of the transition amplitudes for use in a potential model of the heavy-quark wave functions starting with a covariant Feynman-diagram description (Sec. II). The details of the formalism and of the calculations are described in Sec. III. Our numerical results are presented in Sec. IV and the discussion of these results along with our main conclusions is offered in Sec. V.

II. FROM COVARIANT TO NONCOVARIANT TRANSITION AMPLITUDES

We shall start from a Lorentz-covariant description of the bound-state decay process $a(Q\bar{Q})\to b(Q\bar{Q})+h$ and then make contact with the associated noncovariant wave-function description. In the spirit of the phenomenological constituent quark model, we describe the two-gluon emission transition amplitude for $a(P)\to b(P')+g(q_1)+g(q_2)$ in lowest-order perturbation theory. One has then the three Feynman graphs in Fig. 1, along with the three companion graphs, which are not drawn, with the external gluon lines crossed. Let us consider the kinematical notation indicated in Fig. 1 and introduce the momentum-space Bethe-Salpeter amplitudes for the initial $a(P)\to Q(k')+\bar{Q}(-k)$ and final $Q(K')+\bar{Q}(-K)\to b(P')$ states and their corresponding vertex function Γ and its adjoint $\bar{\Gamma}=\gamma_0\Gamma^*\gamma_0$ (suppressing indices a,b for clarity):

$$\Psi(k',k;P)=i\int d^4y\, e^{ik'\cdot y}\langle 0|T[\bar{q}_r(y)q_{r'}(0)]|a(P)\rangle = \left[\frac{1}{\not k'-m}\Gamma(k',k;P)\frac{1}{\not k-m}\right]_{r'r},$$

$$\bar{\Psi}(K',K;P')=i\int d^4y\, e^{-iK'\cdot y}\langle b(P')|T[\bar{q}_s(0)q_{s'}(y)]|0\rangle = \left[\frac{1}{\not K-m}\bar{\Gamma}(K',K;P')\frac{1}{\not K'-m}\right]_{ss'}. \quad (1)$$

The Feynman one-loop integral associated to the sum of the three graphs (a), (b), and (c) of Fig. 1 and their crossed companions is easily found to be

$$G^{(a)}+G^{(b)}+G^{(c)}=-\frac{i}{N_c}\int\frac{d^4k}{(2\pi)^4}\mathrm{Tr}\left[\frac{1}{\not k'-m}\bar{\Gamma}(k',K;P')\frac{1}{\not K-m}V^a(q_1,q_2)\frac{1}{\not k-m}\Gamma(\not k',k;P)\right.$$
$$+\frac{1}{\not k'-m}V^b(q_1,q_2)\frac{1}{\not K'-m}\bar{\Gamma}(K',k;P')\frac{1}{\not k-m}\Gamma(k',k;P)$$
$$\left.+\frac{1}{\not k'-m}V^c(q_1)\frac{1}{\not K'-m}\bar{\Gamma}(K',K;P')V^c(q_2)\frac{1}{\not k-m}\Gamma(k',k;P)+\text{crossed}\right], \quad (2)$$

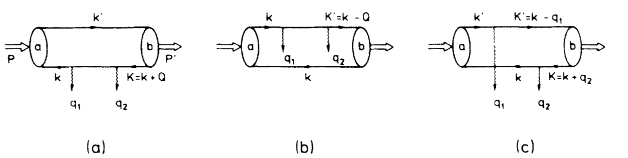

FIG. 1. Direct (a), (b), and interference (c) Feynman diagrams for the bound-state transition amplitudes.

where

$$V^a(q_1,q_2)=\left[\frac{g}{2}\right]^2\lambda_{a_1}\lambda_{a_2}\{\not{\epsilon}_1[(\not{k}+\not{q}_1)-m]^{-1}\not{\epsilon}_2\}\ ,$$

$$V^b(q_1,q_2)=\left[\frac{g}{2}\right]^2\lambda_{a_2}\lambda_{a_1}\{\not{\epsilon}_2[(\not{k}'-\not{q}_1)-m]^{-1}\not{\epsilon}_1\}$$

and

$$V^c(q_i)=\frac{g}{2}\lambda_{a_i}\not{\epsilon}_i$$

are the gluon-quark vertices, λ_a and g the color matrix generators and coupling constant, N_c the number of colors, ϵ_i the gluon polarization vectors, m the quark mass, and the trace is over Dirac spin and color indices. The total amplitude, Eq. (2), is gauge invariant. It is evaluated in the following in the Coulomb gauge, $\mathbf{q}_i\cdot\boldsymbol{\epsilon}_i(\mathbf{q}_i)=0$.

The vertices, Eq. (1), describe the splitting into virtual two-quark systems with the four possible combinations of the sign of the energies, and we wish here to single out the leading $Q\bar{Q}$ component. The crucial step lies in performing the k_0 integration. One physically attractive prescription, motivated by a dispersion theory description of bound-state vertices,[17] is to integrate over k_0 by contour integration while retaining the selected contributions from the single-particle poles with the relevant sign of the energy. For the direct graphs [(a) and (b) in Fig. 1], this is achieved by setting the passive noninteracting quark [graph (a)] or antiquark [graph (b)] on the mass-shell and so leads to the replacement

graph (a):

$$\frac{1}{\not{k}'-m}\to\frac{m}{E_{\mathbf{k}'}}\frac{\Lambda_+(\mathbf{k}')}{k_0'-E_{\mathbf{k}'}+i\epsilon}\to\frac{m}{E_{\mathbf{k}'}}[-2i\pi\delta(k_0'-E_{\mathbf{k}'})]\Lambda_+(\mathbf{k}')\ , \tag{3}$$

graph (b):

$$\frac{1}{\not{k}-m}\to-\frac{m}{E_{\mathbf{k}}}\frac{\Lambda_-(-\mathbf{k})}{k_0+E_{\mathbf{k}}-i\epsilon}\to\frac{m}{E_{\mathbf{k}}}[2i\pi\delta(k_0+E_{\mathbf{k}})]\Lambda_-(-\mathbf{k})\ . \tag{4}$$

Here

$$\Lambda_\pm(\mathbf{k})=\sum_{\text{pol}}\left[\begin{matrix}u(\mathbf{k})\bar{u}(\mathbf{k})\\-v(\mathbf{k})\bar{v}(\mathbf{k})\end{matrix}\right]=\frac{\pm\not{k}+m}{2m}$$

are the Dirac spinors projection operators and $E_{\mathbf{k}}=\sqrt{\mathbf{k}^2+m^2}$.

For the interference graph [graph (c) in Fig. 1], both the quark and antiquark are active and the above identification is not available. One possible prescription to project out the quark-antiquark component, following Blankenbecler and Sugar,[18] is to replace the product of the two Dirac propagators by the two-particle unitarity-cut contribution

graph (c):

$$\frac{1}{(\not{k}'-m)(\not{k}-m)}\to-\frac{m^2}{E_{\mathbf{k}}}\left[2i\pi\delta\left[k_0+\frac{P_0}{2}\right]\right]\times\frac{\Lambda_+(\mathbf{k}')\Lambda_-(-\mathbf{k})}{\frac{1}{4}[P^2-(E_{\mathbf{k}'}+E_{\mathbf{k}})^2]}\ . \tag{5}$$

This amounts to set both the quark and the antiquark off shell, but in a symmetrical way.

If we adopt the above prescriptions and substitute Eqs. (3)–(5) for the propagators in Eq. (2), then the k_0 integrations can be performed easily to yield

$$\begin{aligned}G^{(a)}+G^{(b)}+G^{(c)}=\frac{1}{N_c}\int\frac{d^3k}{(2\pi)^3}\frac{m}{E_{\mathbf{k}}}\mathrm{Tr}\Bigg[&\psi_b^*(\mathbf{k}+\mathbf{Q}/2)[-\bar{v}(-\mathbf{k})V^a(q_1,q_2)v(-\mathbf{K})]\psi_a(\mathbf{k})|_{k_0'=E_{\mathbf{k}'}}\\&+\psi_b^*(\mathbf{k}-\mathbf{Q}/2)[\bar{u}(\mathbf{K})V^b(q_1,q_2)u(\mathbf{k}')]\psi_a(\mathbf{k})|_{k_0=-E_{\mathbf{k}}}\\&-\psi_b^*(\mathbf{k}-\mathbf{Q}_-/2)\left[\bar{u}(\mathbf{K}')V^c(q_1)u(\mathbf{k}')\frac{1}{K_0'-E_{\mathbf{K}'}-i\epsilon}\right.\\&\left.\times\bar{v}(-\mathbf{k})V^c(q_2)v(-\mathbf{K}')\right]\psi_a(\mathbf{k})\Big|_{k_0=-k_0'=-P_0/2}+\text{crossed}\Bigg]\ ,\end{aligned} \tag{6}$$

where $\mathbf{Q}=\mathbf{q}_1+\mathbf{q}_2, \mathbf{Q}_-=\mathbf{q}_1-\mathbf{q}_2$, and the successive terms refer to graphs (a), (b), and (c). Based on the above prescriptions, we have thus obtained a formally noncovariant formula for the transition amplitude where the quantities which satisfy the role of the Schrödinger wave functions are given as

graph (a):

$$\psi_a(\mathbf{k})=-\frac{m}{E_{\mathbf{k}}}\frac{\bar{u}(\mathbf{k}')\Gamma(k',k;P)v(-\mathbf{k})}{k_0+E_{\mathbf{k}}-i\epsilon}\,,$$

$$\psi_b^*(\mathbf{k}+\mathbf{Q}/2)=-\frac{m}{E_{\mathbf{k}}}\frac{\bar{v}(-\mathbf{K})\bar{\Gamma}(k',K;P')u(\mathbf{k}')}{K_0+E_{\mathbf{K}}-i\epsilon}\,, \tag{7a}$$

graph (b):

$$\psi_a(\mathbf{k})=\frac{m}{E_{\mathbf{k}}}\frac{\bar{u}(\mathbf{k}')\Gamma(k',k;P)v(-\mathbf{k})}{k_0'-E_{\mathbf{k}'}+i\epsilon}\,,$$

$$\psi_b^*(\mathbf{k}-\mathbf{Q}/2)=\frac{m}{E_{\mathbf{k}}}\frac{\bar{v}(-\mathbf{k})\bar{\Gamma}(K',k;P')u(\mathbf{K}')}{K_0'-E_{\mathbf{K}'}+i\epsilon}\,, \tag{7b}$$

graph (c):

$$\psi_a(\mathbf{k})=m\frac{\bar{u}(\mathbf{k}')\Gamma(k',k;P)v(-\mathbf{k})}{\frac{1}{4}[M_a^2-(E_{\mathbf{k}}+E_{\mathbf{k}'})^2+i\epsilon]}\,,$$

$$\psi_b^*(\mathbf{k}-\mathbf{Q}_-/2)=-\frac{m}{E_{\mathbf{K}'}}\frac{\bar{v}(-\mathbf{K})\bar{\Gamma}(K',K;P')u(\mathbf{K}')}{K_0+E_{\mathbf{K}}-i\epsilon}\,. \tag{7c}$$

The time components of k and k' are to be evaluated as indicated by Eqs. (3)–(5). By comparing Eqs. (1) and (7), we see that the nonrelativistic wave functions, Eq. (7), appear as the residues of suitable pole contributions for the Bethe-Salpeter amplitudes,[19] Eq. (1), such that the poles locations all coincide in the adiabatic limit with $(-M_a+2E_{\mathbf{k}}-i\epsilon)=0$. While the above wave functions differ slightly in form from one graph to the other, they all become identical when one takes the nonrelativistic and adiabatic $\omega_i \ll k^2/m$ limits. We note that the Blankenbecler-Sugar prescription,[18] if applied also to the direct graphs, would lead to the same answer as the above in the adiabatic limit.

The use of the time-ordered perturbation theory (TOPT) rules from the start would also yield nearly identical formulas to the above, with differences given by terms which vanish in the adiabatic approximation. Naturally, the TOPT rules lead to identical results to the ones obtained by integrating consistently over k_0 via a contour integral over the upper or lower semicircles and picking up all the single-particle poles residues. Let us finally note that our special Blankenbecler-Sugar treatment for the interference graph has the peculiarity that its associated energy denominator reads

$$K_0'-E_{\mathbf{K}'}\simeq -\frac{1}{2}\left[-M_a+2m+2\omega_1+\frac{k^2}{m}\right].$$

Thus it differs from that of the TOPT formula by the replacement $\omega_1\to 2\omega_1$. That the two treatments differ only by nonadiabatic terms should not be surprising. In what follows, we shall retain the dependence on the gluon energies in energy denominators and use the expressions obtained for them in the TOPT treatment.

III. NONRELATIVISTIC AMPLITUDES AND PARTIAL-WAVE PROJECTION

The general formalism of Sec. II is applied to the transitions

$$n\,^3S_1\to n'\,^3S_1+(gg)_{0\pm},\quad n\,^3D_J\to n'\,^3S_1+(gg)_{0\pm}\,,$$
$$n\,^3S_1\to n'\,^1P_1+(gg)_{0\pm},\quad n\,^3P_J\to n'\,^1S_0+(gg)_{0\pm}\,.$$

We shall specialize to the initial-state rest frame $\mathbf{P}=0$, $\mathbf{P}'=-\mathbf{Q}$ and make use of the following approximations in evaluating the vertices V: (1) nonrelativistic approximation for the heavy-quark vertices via an expansion in powers of k/m; (2) neglect of the recoil momentum in the final state (i.e., we set $\mathbf{q}_1=0$ and $\mathbf{q}_2=0$ in the arguments of the final-state wave functions); (3) low excitation energies $\omega_i \ll k$, but still $\omega_i\simeq k^2/m$, i.e., not assuming the adiabatic approximation.

Because of (2) we may then obtain the amplitudes for the *SS*, *SD*, and *PS* transitions by restricting ourselves to the terms of order 0, 2, and 1, respectively, in the quark momentum k. Straightforward but tedious algebra gives the results

$$\begin{aligned}G^{(a/b)}=\frac{g^2}{2N_c}\int\frac{d^3k}{(2\pi)^3}\frac{m}{E_{\mathbf{k}}}\mathrm{Tr}\Bigg\{\psi_b^*(\mathbf{k}\pm\mathbf{Q}/2)\Bigg\{&\frac{1}{(2m)^2e_1}\Bigg[-4\epsilon_1\cdot\mathbf{k}\epsilon_2\cdot\mathbf{k}+2m\left(e_1+\frac{\omega_1^2\pm2\mathbf{k}\cdot\mathbf{q}_1}{m}\right)[\epsilon_1\cdot\epsilon_2\pm i\sigma\cdot(\epsilon_1\times\epsilon_2)]\\
&+e_1\frac{k^2}{2m}\left(\epsilon_1\cdot\epsilon_2\mp\frac{i}{3}\sigma\cdot(\epsilon_1\times\epsilon_2)\right)+(\epsilon_1\cdot\epsilon_2)(\mathbf{Q}\cdot\mathbf{q}_1\pm i\sigma\cdot\mathbf{q}_1\times\mathbf{Q})\\
&-(\epsilon_2\cdot\mathbf{Q})(\epsilon_1\cdot\mathbf{Q}\mp i\sigma\times\mathbf{Q}\cdot\epsilon_1)\pm i\sigma\cdot\mathbf{Q}\epsilon_1\times\epsilon_2\cdot\mathbf{q}_1\Bigg]\\
&+\frac{1}{2m^2e_1}[\mp\epsilon_1\cdot\mathbf{k}(2\epsilon_2\cdot\mathbf{Q}-i\sigma\times\mathbf{Q}\cdot\epsilon_2)\\
&\pm\epsilon_1\cdot\epsilon_2\mathbf{q}_1\cdot\mathbf{k}+i\sigma\cdot\mathbf{k}\epsilon_1\times\epsilon_2\cdot\mathbf{q}_1]+\text{crossed}\Bigg\}\psi_a(\mathbf{k})\Bigg\}\,,\end{aligned} \tag{8}$$

$$G^{(c)}=-\frac{g^2}{2N_c}\int\frac{d^3k}{(2\pi)^3}\frac{m}{E_{\mathbf{k}}}\mathrm{Tr}\left[\psi_b^*(\mathbf{k}-\mathbf{Q}_-/2)\left[\frac{1}{2m^2e_1}(4\epsilon_1\cdot\mathbf{k}\epsilon_2\cdot\mathbf{k}-2i\epsilon_1\cdot\mathbf{k}\epsilon_2\cdot\boldsymbol{\sigma}_{\bar{Q}}\times\mathbf{q}_2\right.\right.$$
$$\left.\left.-2i\epsilon_1\cdot\boldsymbol{\sigma}_Q\times\mathbf{q}_1\epsilon_2\cdot\mathbf{k}-\epsilon_1\cdot\boldsymbol{\sigma}_Q\times\mathbf{q}_1\epsilon_2\cdot\boldsymbol{\sigma}_{\bar{Q}}\times\mathbf{q}_2)+\text{crossed}\right]\psi_a(\mathbf{k})\right], \tag{9}$$

where by crossed we always mean the gluon crossing terms obtained by the interchange of indices 1 and 2. We denote $e_i=(B_a+\omega_i+\mathbf{k}^2/m)$, $B_a=-M_a+2m$ (negative of the excited state binding energy), $\omega_i=q_i^0$ and

$$\boldsymbol{\sigma}=\begin{bmatrix}\boldsymbol{\sigma}_{\bar{Q}}=\boldsymbol{\sigma}^T\\ \boldsymbol{\sigma}_Q=\boldsymbol{\sigma}\end{bmatrix}$$

are the quark and antiquark Pauli spin matrices. On the right-hand side of Eq. (8), the seagull contactlike term, which appears as the second term inside the large brackets, is an off-shell contribution where the $Q(\bar{Q})$ propagates as a virtual $\bar{Q}(Q)$ in the time interval between emission of the first and second gluons.

We shall use the helicity formalism to describe the decomposition of the two-gluon states on partial waves of good angular momentum and space parity. Applying successively the standard angular momentum decomposition formula of Jacob and Wick and its inverse, we obtain

$$\langle b;\mathbf{q}_1\lambda_1\mathbf{q}_2\lambda_2|G|a\rangle=\sum_{jm}\frac{2j+1}{4\pi}\mathcal{D}^j_{m\lambda_1-\lambda_2}(\mathbf{q}^*)\int d\Omega_{\mathbf{q}'^*}\mathcal{D}^{j*}_{m\lambda_1-\lambda_2}(\mathbf{q}'^*)\langle b;\mathbf{q}_1\lambda_1\mathbf{q}_2\lambda_2|G|a\rangle , \tag{10}$$

where λ_i are the gluons helicities, $\mathcal{D}$ are the rotation matrices and we have omitted the Wigner matrices which effect on the gluons state functions the Lorentz-boost transformation $\mathbf{Q}\to\mathbf{Q}^*$ from the laboratory frame to the c.m. frame of the two gluons $\mathbf{Q}^*=0$. These unitary transformations amount to linear bases transformations of the polarization states and hence are irrelevant if one is interested, as we are, in polarization-independent observables. The star will always be used to identify the kinematic variables in the two-gluon c.m. frame. We note that although the derivation of Eq. (10) involves as an intermediate step the use of the two-gluon c.m. frame, the Lorentz invariance of the transition matrix element G permits us to deal with it in terms of the expression of G appearing in Eq. (6) in the laboratory frame.

The transition rate summed over the gluons spatial orientations and polarizations is now obtained by multiplying the squared transition amplitude with the three-body phase-space volume and reads

$$d\Gamma=\frac{(2\pi)^4}{2M_a}\delta^4(P-P'-q_1-q_2)\frac{d^3\mathbf{P}'}{(2\pi)^3 2E_b}\prod_{i=1,2}\frac{d^3q_i}{(2\pi)^3 2\omega_i}\sum_{\lambda_i=\pm1}|G|^2$$
$$=\frac{\pi}{2(2\pi)^5}WQ\sum_{P=\pm\lambda_1}\sum_{\lambda_1\lambda_2}\sum_{jm}\left|\frac{2j+1}{4\pi\sqrt{2}}\int d\Omega_{\mathbf{q}'^*}\mathcal{D}^{j*}_{m\lambda_1-\lambda_2}(\mathbf{q}'^*)\langle b;(\mathbf{q}_1\lambda_1\mathbf{q}_2\lambda_2)^P|G|a\rangle\right|^2 d\Omega_Q dW , \tag{11}$$

where we have integrated over $\Omega_{\mathbf{q}^*}$ by invoking the orthogonality of the rotation matrices, absorbed a factor $1/4M_aM_b$ (assuming $M_a\simeq M_b$) so as to deal with bound-state wave functions normalized as $\langle a|a\rangle=1$ and considered a linear basis transformation to the good space-parity states

$$|(\mathbf{q}_1\lambda_1\mathbf{q}_2\lambda_2)^{\pm}\rangle=(1/\sqrt{2})(|\mathbf{q}_1\lambda_1\mathbf{q}_2\lambda_2\rangle\pm|\mathbf{q}_1-\lambda_1\mathbf{q}_2-\lambda_2\rangle) ,$$

using the fact that opposite-parity states do not interfere.

The transformation from the laboratory to the gluons c.m. frame involves the Lorentz boost of velocity $\beta=Q/\Delta$, $\gamma=(1-\beta^2)^{-1/2}=\Delta/W$ parallel to $\mathbf{Q}$ where $Q=|\mathbf{Q}|$, $\Delta=M_b-M_a=\omega_1+\omega_2$, $W^2=(q_1+q_2)^2=\Delta^2-Q^2$. Exploiting the rotational invariance of the matrix element $\langle b|G|a\rangle$, we shall evaluate it by making the convenient choice of setting the three-axis along $\mathbf{Q}$, it being understood that $\mathbf{Q}$ must be reinstated when carrying the integration of Eq. (11). (The only vectors left out besides $\mathbf{Q}$ are the spin operators $\boldsymbol{\sigma}_Q\pm\boldsymbol{\sigma}_{\bar{Q}}$, so that once one sums over the polarizations there is no dependence left on the orientations of $\mathbf{Q}$.) The kinematics is completely fixed once one is given W and Δ and one fixes one additional variable, which could be, for example, the angular variable x in $\mathbf{q}_1\cdot\mathbf{q}_2$ or x^* in $\mathbf{Q}\cdot\mathbf{q}_1^*$. Thus, denoting by θ_i, ϕ_i the spherical coordinates of the gluons $g(\mathbf{q}_i)$, we have the useful connection formulas

$$\omega_i=\frac{\Delta}{2}(1\pm\beta x^*)=\frac{\Delta}{2}\left[1\pm\left[1-\frac{2W^2}{\Delta^2(1-x)}\right]^{1/2}\right],\quad x_i=\frac{\beta\pm x^*}{1\pm\beta x^*},\quad \omega_i x_i=\frac{\Delta}{2}(\beta\pm x^*) ,$$
$$x^*=\frac{\omega_1-\omega_2}{Q},\quad x=x_1x_2+\xi_1\xi_2\cos(\phi_1-\phi_2) , \tag{12}$$

where $x_i = \cos\theta_i$, $\xi_i = \sin\theta_i$, $x = \cos\theta = \mathbf{q}_1 \cdot \mathbf{q}_2 / \omega_1\omega_2$, $x^* = \cos\theta^* = 2\mathbf{Q}\cdot\mathbf{q}_1^* / QW$ $(i=1,2)$. The following kinematical properties are easily inferred from Eq. (12) and the formula $W^2 = 2\omega_1(\Delta - \omega_1)(1-x)$. (1) For fixed ω_1, W increases monotonically in $(0,\Delta)$ as x varies in $(1,-1)$. (2) For fixed x, W increases then decreases with increasing ω_1 as it passes $\omega_1 = \Delta/2$. (3) For fixed W, when x varies in $(1-2W^2/\Delta^2, -1)$, ω_1 varies in $(\Delta - Q/2, \Delta + Q/2)$.

Based on the dominance for the light hadrons of the low partial waves, especially $j=0$ waves, we shall truncate the partial-wave sum in Eq. (11) to the lowest angular momentum $j=0$. Some useful formulas needed in the projection of the two-gluon states are

$$\epsilon_{-1}^{(\lambda=\pm 1)}(\mathbf{q}_1) = -\frac{1 \pm x_1}{2}, \quad \epsilon_{+1}^{(\lambda=\pm 1)}(\mathbf{q}_1) = -\frac{1 \mp x_1}{2}, \quad \epsilon_0^{(\lambda=\pm 1)}(\mathbf{q}_1) = \pm \frac{\xi_1}{\sqrt{2}} e^{\pm i\phi_1},$$

$$(\boldsymbol{\epsilon}_1 \cdot \boldsymbol{\epsilon}_2)^{(0^+,0^-)} = \left[-\frac{1-x}{\sqrt{2}}, 0 \right], \quad (\boldsymbol{\epsilon}_1 \times \boldsymbol{\epsilon}_2)^{(0^+,0^-)} = \left[0, \frac{i(x_1 - x_2)\mathbf{Q}}{Q\sqrt{2}} \right],$$

$$[(\boldsymbol{\epsilon}_1 \times \boldsymbol{\epsilon}_2)^{(2)}_{-2}]^{(0^+,0^-)} = \frac{1}{2\sqrt{2}} [1 + x_1 x_2, -(x_1 + x_2)],$$

$$[(\boldsymbol{\epsilon}_1 \times \boldsymbol{\epsilon}_2)^{(2)}_{0}]^{(0^+,0^-)} = \frac{1}{2\sqrt{3}} [1 - x_1 x_2 + 2\xi_1\xi_2, 0],$$

$$[(\boldsymbol{\epsilon}_1 \cdot \mathbf{a})(\boldsymbol{\epsilon}_2 \cdot \mathbf{b})]^{0^+} = \frac{1}{2\sqrt{2}} \Bigg[(1 + x_1 x_2)(a_x b_x - a_y b_y) - (1 - x_1 x_2)(a_x b_x + a_y b_y)$$
$$- 2\frac{a_z}{\omega_1}(-b_y q_{1y} + x_2 b_x q_{1x}) - 2\frac{b_z}{\omega_2}(a_y q_{2y} + x_1 a_x q_{2x}) + 2 a_z b_z \xi_1 \xi_2 \Bigg],$$

$$[(\boldsymbol{\epsilon}_1 \cdot \mathbf{a})(\boldsymbol{\epsilon}_2 \cdot \mathbf{b})]^{0^-} = \frac{i}{2\sqrt{2}} \Bigg[(x_1 + x_2)(a_x b_y + a_y b_x) + (x_1 - x_2)(a_x b_y - a_y b_x)$$
$$- 2\frac{a_z}{\omega_1}(b_y q_{1x} + x_2 b_x q_{1y}) - 2\frac{b_z}{\omega_2}(a_y q_{2x} - x_1 a_x q_{2y}) \Bigg]. \tag{13}$$

We also quote the nonvanishing matrix elements with respect to the intrinsic spin of the quarks in the spin-coupled basis (SS_z): $\langle 11 | (\sigma_Q - \sigma_{\bar{Q}})_z | 11 \rangle = 2$, $\langle 00 | (\sigma_Q + \sigma_{\bar{Q}})_z | 10 \rangle = 2$.

The basic formulas for the differential transition rates are listed below.

${}^3S_1 \to {}^3S_1$:

$$\frac{d\Gamma^{0^+}}{dW} = \frac{\alpha_s^{E2} W}{648\pi Q} \left| \int_{\omega_-}^{\omega_+} d\omega_1 (1-x) \left\langle 8\frac{\mathbf{k}^2}{m^2} \left[\frac{1}{e_1} + \frac{1}{e_2} \right] \right\rangle \right|^2,$$

$$\frac{d\Gamma^{0^-}}{dW} = \frac{\alpha_s^E \alpha_s^M W}{648\pi Q} \frac{8}{3} \left| \int_{\omega_-}^{\omega_+} d\omega_1 \left\langle \frac{3}{2m^2 e_1} \left[(x_1 - x_2)[2\omega_1^2 + (\omega_1^2 + \omega_1\omega_2 x)(1 + \tfrac{2}{3} k\, d/dk)] \right.\right.\right.$$
$$\left.\left.\left. + \frac{Q\Delta}{6}(x - x_1 x_2)(1 + x^*) k \frac{d}{dk} \right] \right\rangle + \text{crossed} \right|^2, \tag{14}$$

${}^3D_J \to {}^3S_1$:

$$\frac{d\Gamma^{0^+}}{dW} = \frac{\alpha_s^{E2} W}{648\pi Q} \frac{3}{25} \left[\left| \int_{\omega_-}^{\omega_+} d\omega_1 (1 + x_1 x_2) \left\langle \frac{8k^2}{m^2} \left[\frac{1}{e_1} + \frac{1}{e_2} \right] \right\rangle \right|^2 \right.$$
$$\left. + \frac{1}{3} \left| \int_{\omega_-}^{\omega_+} d\omega_1 (1 + 2x - 3x_1 x_2) \left\langle \frac{8k^2}{m^2} \left[\frac{1}{e_1} + \frac{1}{e_2} \right] \right\rangle \right|^2 \right],$$

$$\frac{d\Gamma^{0^-}}{dW} = \frac{\alpha_s^{E2} W}{648\pi Q} \frac{3}{25} \left[\left| \int_{\omega_-}^{\omega_+} d\omega_1 (x_1 + x_2) \left\langle \frac{8k^2}{m^2} \left[\frac{1}{e_1} + \frac{1}{e_2} \right] \right\rangle \right|^2 \right], \tag{15}$$

${}^3S_1 \to {}^1P_1$:

$$\frac{d\Gamma^{0^+}}{dW}=\frac{\alpha_s^E\alpha_s^M W}{81\pi Q}\left[\left|\int_{\omega_-}^{\omega_+}d\omega_1\left\langle\frac{k}{2m^2e_1}(Q+\gamma_1+\gamma_2)\right\rangle+\text{crossed}\right|^2+\left|\int_{\omega_-}^{\omega_+}d\omega_1\left\langle\frac{k}{2m^2e_1}(Q+\gamma_1-\gamma_2)\right\rangle+\text{crossed}\right|^2\right],$$

$$\frac{d\Gamma^{0^-}}{dW}=\frac{4\alpha_s^E\alpha_s^M W}{81\pi Q}\left[\left|\int_{\omega_-}^{\omega_+}d\omega_1\left\langle\frac{k(\alpha+\alpha')}{2m^2e_1}\right\rangle+\text{crossed}\right|^2+2\left|\int_{\omega_-}^{\omega_+}d\omega_1\left\langle\frac{k(\alpha+\beta_2+\beta_2')}{2m^2e_1}\right\rangle+\text{crossed}\right|^2+2\left|\int_{\omega_-}^{\omega_+}\left\langle\frac{k(\beta_1+\beta_1')}{2m^2e_1}\right\rangle+\text{crossed}\right|^2\right], \tag{16}$$

${}^3P_J \to {}^1S_0$:

$$\frac{d\Gamma^{0^+}}{dW_{J=1}}=\frac{\alpha_s^E\alpha_s^M W}{81\pi Q}\left|\int_{\omega_-}^{\omega_+}d\omega_1\left\langle\frac{k}{2m^2e_1}(Q+\gamma_1-\gamma_2)\right\rangle+\text{crossed}\right|^2,$$

$$\frac{d\Gamma^{0^-}}{dW_{J=\binom{0}{2}}}=\frac{4\alpha_s^E\alpha_s^M W}{81\pi Q(2J+1)}\left[\begin{bmatrix}1\\2\end{bmatrix}\left|\int_{\omega_-}^{\omega_+}d\omega_1\left\langle\frac{k(\alpha+\alpha')}{2m^2e_1}\right\rangle+\text{crossed}\right|^2+4\begin{bmatrix}1\\ \frac{1}{2}\end{bmatrix}\left|\int_{\omega_-}^{\omega_+}d\omega_1\left\langle\frac{k(\alpha+\beta_2+\beta_2')}{2m^2e_1}\right\rangle+\text{crossed}\right|^2+12\begin{bmatrix}0\\1\end{bmatrix}\left|\int_{\omega_-}^{\omega_+}d\omega_1\left\langle\frac{k(\beta_1+\beta_1')}{2m^2e_1}\right\rangle+\text{crossed}\right|^2\right]. \tag{17}$$

Here $\omega_\pm=(\Delta\pm Q)/2$ and we have changed the integration variable from x^* to ω_1 using Eq. (12), $dx^*=(2/Q)d\omega_1$. There should hopefully arise no confusion between the physical kinematical variables and the corresponding integration variables involved in the angular momentum projection which we have denoted by the same symbols $(\omega_1,x,\ldots)$. The following notation is used for the expectation values with respect to the appropriately normalized radial wave functions:

$$\langle O\rangle=\int_0^\infty dk\,k^2R_b^*(k)OR_a(k)\,,\qquad \int_0^\infty dk\,k^2R_b^*(k)R_a(k)=\delta_{ab}\,; \tag{18}$$

and for the factors appearing in the reduction of the matrix elements for the various transitions:

$$\alpha=\frac{1}{Q\sqrt{2}}x^*(1-x)(\omega_1^2+\omega_1\omega_2x)\,,\qquad \alpha'=\frac{\xi_1\xi_2}{2\sqrt{2}}[\omega_2(1-x_2)+\omega_1(1-x_1)]\,; \tag{19}$$

$$\beta_1+\beta_1'=\frac{1}{2\sqrt{2}}[(x_2+x_1)(Q+\omega_2x_2+\omega_1x_1)-\tfrac{1}{2}(\omega_2x_1\xi_2+\omega_1x_2\xi_1)]\,,$$
$$\beta_2+\beta_2'=\frac{1}{2\sqrt{2}}[(x_2-x_1)(Q+\omega_2x_2-\omega_1x_1)+\tfrac{1}{2}(\omega_2x_1\xi_2+\omega_1x_2\xi_1)]\,; \tag{20}$$

$$\gamma_1=[\omega_2x_2+\omega_1x_1-\tfrac{1}{2}(\omega_2\xi_2^2+\omega_1\xi_1^2)]\,,\qquad \gamma_2=[x_1x_2(Q+\omega_2x_2+\omega_1x_1)+\tfrac{1}{2}(\omega_2\xi_2^2x_1+\omega_1\xi_1^2x_2)]\,. \tag{21}$$

In obtaining the above formulas for the projected transition rates an extra factor $\frac{1}{2}$ has been inserted in order to account for the indistinguishability of the gluons and thus to compensate for their double counting in the projected states. Accordingly, our partial-wave integrated rates are to be calculated as $\Gamma^{0\pm}=\int dW(d\Gamma/dW)$.

The following comments are useful to note in connection with the above results.

(1) The multipolarities of the gluons which are involved in the leading contributions retained in the formulas above are, for the SS and SD transitions, $E1$-$E1$ in the 0^+ two-gluon channel and $E1$-$M2$ (direct graphs) and $M1$-$M1$ (interference graphs) in the 0^- channel. For the SP transitions, the multipolarities are $E1$-$M1$ in both channels. The conservation of angular momentum and of space and charge-conjugation parities fixes the allowed values of the orbital momentum L for the motion of the gluons relative to the recoiling heavy-quark system. Noting that $\mathbf{j}_a=\mathbf{j}_b+\mathbf{L}+\mathbf{j}$, the following correspondence relations are seen to hold for our $j=0$ case:

$$\begin{aligned}
&{}^3S(1^-)\to{}^3S(1^-)+0^\pm:\begin{bmatrix}E1\text{-}E1\\ E1\text{-}M2\oplus M1-M1\end{bmatrix}:L=\begin{bmatrix}0,2\\1\end{bmatrix},\\
&{}^3D(1^-)\to{}^3S(1^-)+0^\pm:(E1\text{-}E1):L=\begin{bmatrix}0,2\\1\end{bmatrix},\\
&{}^3S(1^-)\to{}^1P(1^+)+0^\pm:(E1\text{-}M1):L=\begin{bmatrix}1\\0,2\end{bmatrix},\\
&{}^3P\begin{bmatrix}1^+\\0^+,2^+\end{bmatrix}\to{}^1S(0^-)+0^\pm:(E1\text{-}M1):L=\begin{bmatrix}1\\0,2\end{bmatrix}.
\end{aligned} \tag{22}$$

The upper and lower entries correspond to the $0^\pm$ channels. We note that the multipolarity L determines the threshold behavior of the amplitudes to be Q^{2L+1} as $Q \to 0$, $W \to \Delta$.

Anticipating the distinction to be made between electric and magnetic multipoles, which will play an important role in the following discussion, we have introduced in Eqs. (14)–(17) distinct notations g_E and g_M for the electric and magnetic-color coupling constants and defined accordingly $\alpha_s^E = g_E^2/4\pi$, $\alpha_s^M = g_M^2/4\pi$.

(2) In the $S \to S + 0^-$ case a remarkable cancellation of the off-shell effects takes place, on one hand, through the direct and crossed gluon contributions and, on the other hand, through the orthogonality relation between the initial- and final-state wave functions, so the leading-order nonvanishing contributions which appear in Eq. (14) are of order ω_i^2/m^2. We note that the analog of this strong suppression of the 0^- gluons emission amplitude relative to the 0^+ is not at all apparent in the multipole expansion approach.

(3) The fact that the $S \to S + 0^-$ amplitude arises from terms of quadratic order in the gluon energies suggests that one should also take into account the recoil corrections associated with the dependence on the gluons momentas in the final-state wave functions. The approximate evaluation of these contributions, which is obtained by Taylor expanding the wave functions, yields the terms appearing in Eq. (14) with the derivative d/dk.

(4) The unpolarized transition rates have been obtained by taking free incoherent sums over the initial- and final-state angular momentum projections λ_a, λ_b with respect to the quantization axis $\mathbf{Q}$. The diagonal matrix elements $\lambda_a = \lambda_b$ behave as W^2 while the off-diagonal ones are generally finite as $W \to 0$. For the SS transitions, the leading operators are spin independent so in the leading nonrelativistic order only the diagonal terms are involved and the transition amplitude has a W^2 behavior. For the DS transitions, Eq. (15), the off-diagonal matrix elements $|\lambda_b - \lambda_a| = 2$ are responsible for the term $(1 + x_1 x_2)$ in the 0^+ channel and for the term $(x_1 - x_2)$ in the 0^- channel, both resulting in a constant transition amplitude as $W \to 0$. As a result of this the $D \to S + 0^\pm$ transition rates are of the same magnitude unlike the $S \to S + 0^\pm$ rates for which the ratio of 0^- to 0^+ is roughly 10^{-3}. For the PS transitions, the contributions in the 0^+ case are purely off diagonal in the angular momentum projections, hence finite as $W \to 0$. On the other hand, both diagonal and off-diagonal contributions are present in the 0^- channel, the former being responsible for the terms involving the quantity α, Eq. (19).

The general behavior at small W can also be conveniently analyzed in the helicity formalism, as first discussed by BLMN (Ref. 5). Let λ_a, λ_b denote initial and final helicities of the heavy-quark states. Let also λ_1, λ_2 denote, as before, the gluons helicities in their common rest frame so that we need not introduce the Wigner rotations associated to the boost β from the laboratory frame. The first step in the reasoning consists of using the crossing relation to relate the three-body $a \to b + g + g$ decay amplitude to the two-body $a + \bar{b} \to g + g$ scattering amplitude and in invoking the known threshold behavior at $W \to 0$ of the latter, as deduced via an analysis of kinematical singularities. This yields

$$\langle \lambda_1 \lambda_2 | G | \lambda_b \lambda_a \rangle \simeq \langle \lambda_b ; \lambda_1 \lambda_2 | G | \lambda_a \rangle \approx W^{|-\epsilon(\lambda_a - \lambda_b) + (\lambda_1 + \lambda_2)|} , \tag{23}$$

where $\epsilon = \pm 1$ and the equalities hold up to constant factors and to analytic continuation in the W complex plane. By writing then the Dalitz basis[20] partial-wave decomposition of the three-particle state,

$$\langle \lambda_b ; \lambda_1 \lambda_2 | G | \lambda_a \rangle = \sum_{jm} \mathcal{D}^j_{m\lambda_1 - \lambda_2}(\Omega_{\mathbf{q}^*}) \mathcal{D}^{J_a}_{m - \lambda_b \lambda_a}(\Omega_{-\mathbf{Q}}) \times \langle \lambda_b ; \lambda_1 \lambda_2 | G^{jm}(W) | \lambda_a \rangle , \tag{24}$$

one sees that the projection $j = 0$ forces $m = 0$, $\lambda_1 = \lambda_2$ but imposes no relations between λ_a and λ_b. The off-diagonal terms $\lambda_a \neq \lambda_b$, which arise whenever a nonvanishing orbital angular momentum L exists between the gluon pair and the recoiling heavy-quark state, are not necessarily absent. These terms do not vanish with W whereas the diagonal terms always vanish like W^2, as one verifies in Eq. (23).

Our formula, Eq. (15), for the DS transition differs from that of BLMN (Ref. 5) in that ours is an incoherent sum of two terms while theirs contains one term only. The difference appears to be due to the special prescription used by them which involves both the projection $j = 0$ and the restriction to diagonal matrix elements in the angular momentum projections, while we do not discard the off-diagonal matrix elements.

(5) The scaling dependence with quark mass and size parameters are easily deduced by inspection of Eqs. (14)–(17):

$$\left\{ \frac{d\Gamma}{dW} \right\}^{0^\pm} = \begin{cases} \dfrac{1}{m^4 a^2} \simeq \dfrac{1}{m^2} & \text{for } SS, DS, PP, \\[2ex] \dfrac{1}{m^4 a} \simeq \dfrac{1}{m^3} & \text{for } PS, \end{cases} \tag{25}$$

where the bound-state size parameter has been set approximately as $a \simeq m^{-1}$.

(6) The formulas in Eq. (15) for the ${}^3D_J \to {}^3S_1$ transition rates are independent of the initial-state spin J. The first formula in Eq. (14) applies also to the transition $P_J \to P_J + 0^+$ in the approximation where one retains the scalar part only of the transition operator.

IV. NUMERICAL RESULTS

We have evaluated the formulas (14)–(17) for the transition rates by numerical integration. Our results for the mass spectra of the emitted hadrons are shown in Figs. 2 and 3 and the comparison with data is given in Fig. 4. The results for the integrated rates are listed in Tables I and II where they are compared with the available experimental data and also with the predictions of the mul-

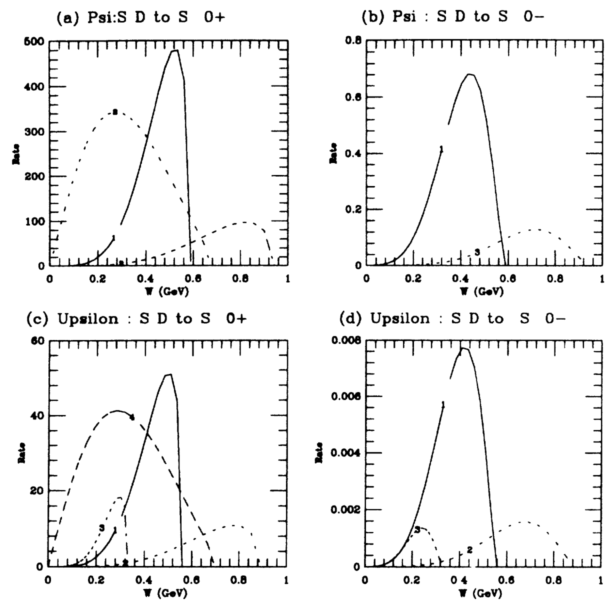

FIG. 2. *SS* and *DS* differential transition rates for emission of light hadrons of invariant mass W and $J^{PC}=0^+$ (left) and 0^- (right). The labels 1,2,3 on curves in (a) and (b) for the J/ψ system correspond to $1=2S\rightarrow 1S$, $2=1D\rightarrow 1S$, $3=3S\rightarrow 1S$. The curve labels 1,2,3,4 in the bottom [(c),(d)] for the Υ system correspond to $1=2S\rightarrow 1S$, $2=3S\rightarrow 1S$, $3=3S\rightarrow 2S$, $4=1D\rightarrow 1S$.

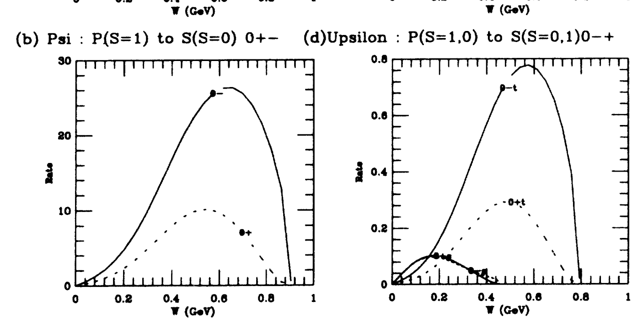

FIG. 3. Differential transition rates for the singlet (triplet) P states to triplet (singlet) S states for emission of light hadrons in $J^P=0^+,0^-$ states with invariant mass W. (a) and (b) for the J/ψ system refer to the singlet and triplet P transitions: $1\,{}^1P_1\rightarrow 1\,{}^3S_1$ (a) and $2\,{}^3P_{J=\binom{0}{1}}\rightarrow 1\,{}^1S_0+\binom{0^-}{0^+}$ (b). (c) and (d) for the Υ system refer to $2\,{}^1P_1\rightarrow 1\,{}^3S_1+0^-$ (c) and $1\,{}^3P_{J=\binom{0}{1}}\rightarrow 1\,{}^1S_0+\binom{0^-}{0^+}$ [rightmost curves in (d)], $3\,{}^3S_1\rightarrow 1\,{}^1P_1+0^{\mp}$ [leftmost curves in (d)], using the label t for triplet P and s for singlet P.

tipole approach both in the soft-pion local version of VZNS (Refs. 9–12) and in two nonlocal versions of the Kuang-Yan model.[13,14]

We have made use of a harmonic-oscillator potential for the $Q\bar{Q}$ potential $V(r)=\frac{1}{4}m\omega^2r^2$ (m=quark mass) with $\omega=0.3$ GeV, as found approximately by adjusting to the splitting $M(2S)-M(1S)=2\omega$. The harmonic-oscillator choice is motivated by the wish to retain simple analytic expressions for the wave functions. The discrepancies with respect to a realistic potential calculation do not exceed on the average a few 10%, as we checked by comparing some of our results for *SS* transitions with those of BLMN (Ref. 5). Thus, our simple-minded wave functions should be sufficiently reliable for a semiquantitative analysis.

The quark masses were set to $m_c=1.7$ GeV, $m_b=5.0$ GeV. We have also set the binding energy parameter $B_a=-M_a+2m=0$ in order to avoid the technical embarrassment of dealing with singular energy denominators.

In the simplest version of the two-gluon emission model as developed so far we need to specify one explicit parameter, the color coupling constant, as well as two other implicit constant parameters which serve to parametrize the probabilities for the hadronization amplitudes in the two channels relevant to low-energy hadrons: $(gg)_{0^+}\rightarrow\pi^+\pi^-\oplus\pi^0\pi^0$ and $(gg)_{0^+}\rightarrow\eta\oplus\pi^0$. The underlying assumption here is that these amplitudes can be regarded as local, energy-independent amplitudes. Now, it appears very clearly on comparing our results for the rates with experiment (see columns A in Tables I and II) that some

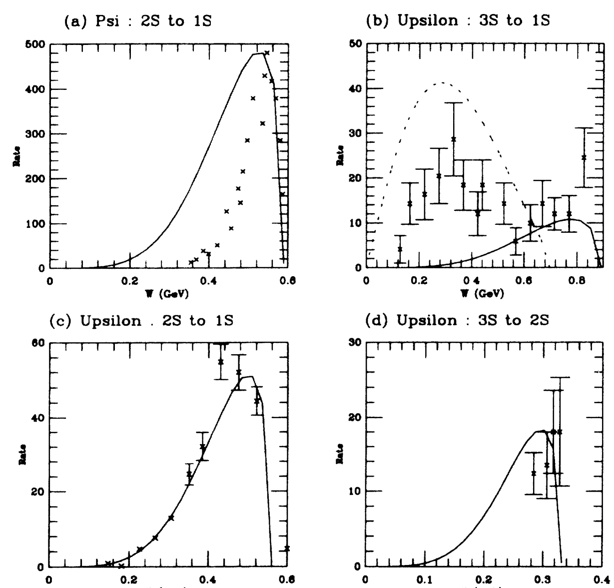

FIG 4. Differential transition rates $d\Gamma/dW(S\rightarrow S+\pi\pi)$. The experimental data points (extracted for charmonium from a visual fit of the histogram in Ref. 5 and for bottomonium from Ref. 2) have been normalized by a multiplicative constant factor determined so as to match data with theoretical predictions at the large W side. The dashed curve in (b) refers to the theoretical prediction for $1\,{}^3D_1\rightarrow 1\,{}^3S_1+(gg)_{0^+}$.

adjustment of the hadronization amplitudes is needed which should enable us to discriminate between the 0^+ and 0^- cases. Rather than introducing new independent parameters for each transition, one prescription which is naturally suggested by our results is to associate different values for the electric and magnetic gluon-quark couplings. This could, for example, describe a situation where the heavy quarks acquire some anomalous magnetic moment, as was initially observed by Kuang and Yan.[13] We have already indicated above how this prescription can be implemented in practice by introducing distinct electric and magnetic-color coupling constants.

If we adjust our color coupling constants so as to reproduce the two observed transitions in the J/ψ system, $\Gamma(\psi'+\psi+\pi\pi)=121.5\pm23.5$ keV, $\Gamma(\psi'\to\psi+\eta) =6.6\pm1.5$ keV, the following values of the coupling constants are obtained: $\alpha_s^E\simeq 1.12$, $\alpha_s^M\simeq 18$.

One should attach no more than semiquantitative significance to the above assignments since the adjusted values in our simple application of the model possibly subsume important corrections from other sources. The most important correction should be that arising from the kinematical phase-space effects. For the $\pi\pi$ case, the size of the corrections associated to the shifted threshold $W=2m_\pi$ depend sensitively on the transition type. They do not exceed a few % for the SS transitions, owing to their suppression at low W, but induce large reduction factors of order 2 to 8 in the DS and PS transitions depending on the extent of their peaking at low W and on the available energy Δ. (The precise amount can be easily determined by comparing in Tables I and II the predictions in columns A and B after the removal of the normalization factors from the coupling constants.)

By contrast, the two-gluon phase space is certainly a very poor representation for the η meson but the corresponding error on the rate is unfortunately difficult to estimate. Also, because of the small value of the η-meson emission amplitude in our approach, the uncertainties from the various technical approximations (choice of wave functions, nonrelativistic expansion, . . .) should have larger effects. Thus, for example, if we discard the recoil correction terms in Eq. (14) involving the derivative on wave functions, we would find that the assigned value of a_s^M must be increased by a factor 2 to 3.

The 0^- is a two-channel $\eta\oplus\pi^0$ system. The π^0 is essentially coupled via isospin breaking effects which are generally small at the level of our present study. The π^0 channel becomes interesting when the η channel is energetically closed. To obtain the π^0 amplitude in this case we need some explicit assumption for the hadronization amplitude. Following standard phenomenological motivations, we shall consider the possibility that both η and π^0 two-gluon annihilation amplitudes are well described perturbatively in terms of the quark triangle loop graph. We assume furthermore that the effective coupling to gluons is local and dominated by the axial anomaly operator $\omega=(g^2/16\pi^2)\,\mathrm{Tr}(G_{\mu\nu}\tilde{G}^{\mu\nu})$. (A similar con-

TABLE I. Hadronic transition rates Γ in keV in the $c\bar{c}$ system. For each initial- and final-state configuration, the first line gives the $0^+=\pi^+\pi^-\oplus\pi^0\pi^0$ rates and the second line the $0^-=\eta\oplus\pi^0$ rates. The predictions found in this work are presented in an unrenormalized version (column A) ($\alpha_s^E=1$, $\alpha_s^M=1$) and in a renormalized version (column B) enclosed inside brackets which incorporates three corrections: (1) hadronization probability $\alpha_s^E=1.12$, $\alpha_s^M=18$, i.e., relative to column A an extra factor $\alpha_s^E\alpha_s^M\simeq 20$ for $S\to S+0^-$ and $P\to S+0^\pm$; (2) phase space with threshold value $W=2m_\pi$; (3) extra factor 9×10^{-4} in Eq. (26) for π^0 emission. The predictions found in the multipole approach are labeled by (a) for the VZSN low-energy model[9,12] and (b) for the Kuang-Yan partonic model.[13,14] The experimental data are from Ref. 2 and from the compilation.[21]

Transition	Δ (MeV)	This work A	This work B	Multipole	Expt.
$\psi'(2S)\to\psi(1S)+0^\pm$	589	97.2	[120]		121.5±23.5
		0.36	[6.3]	8.5–10.9[a]	6.6±1.5
$1^3D_J\to\psi(1S)+0^\pm$	673	376	[110]		
		146	[109]		
$\psi''(3S)\to\psi(1S)+0^\pm$	943	34	[43.6]		
		0.16	[3.1]		
$2P_J\to1P_J+0^+$	489	38	[45]		
$1^1P_1\to\psi(1S)+0^\pm$	414 (π^0)	18.4	[52.6]		
		18.6	[0.61×10^{-1}]	2[b]	
$\psi'(2S)\to1^1P+0^-$	175 (π^0)	0.25×10^{-1}	[0.43×10^{-3}]	0.8[b]	
$1^3P_1\to\eta_c(1S)+0^+$	414	1.85	[17.4]		
$1^2P_{J=\binom{0}{2}}\to\eta_c(1S)+0^-(\pi^0)$		6.0	[0.69×10^{-1}]		
		19.3	[0.38×10^{-1}]		
$2^3P_1\to\eta_c(1S)+0^+$	903	4.5	[82]		
$2^3P_{J=\binom{0}{2}}\to\eta_c(1S)+0^-$		13	[248]		
		34	[447]		

clusion is also involved in the multipole approach.[9]) By direct calculation of the triangle graph or by application of the low-energy soft-meson theorem based on the anomaly in the flavor singlet axial-vector current[22] one predicts that the ratio of η to π^0 amplitudes is

$$\frac{\langle 0|\omega|\eta\rangle}{\langle 0|\omega|\pi^0\rangle}=\frac{4}{3\sqrt{3}}\frac{m_s-\overline{m}}{m_d-m_u}\simeq 34\ ,$$

where $\overline{m}=(m_u+m_d)/2$ and the numerical estimate uses the values of quark masses $(m_u,m_d,m_s)=4.2,7.5,150$ MeV. To determine the branching ratio for π^0 to η emission in the cases where the η channel is open, one must still account for the dependence on the meson momentum expected on the basis of the one-body phase-space factor and of relativistic invariance. This gives

$$r=\frac{\Gamma(a\to b+\pi^0)}{\Gamma(a\to b+\eta)}=\left[\frac{m_\pi^2\sqrt{3}(m_d-m_u)}{m_\eta^2(m_d+m_u)}\right]^2x^3$$
$$\simeq 9\times 10^{-4}x^3\ , \qquad (26)$$

where $x=p_\pi/p_\eta$ is the ratio of the mesons laboratory momenta and for the numerical estimate we have used the pseudoscalar-meson mass formulas to express the strange-quark mass. Typical values for the kinematical factor x^3 in Eq. (26) are 20:5:2 for $\Delta\simeq 600{:}700{:}900$ MeV, so the π^0 channel is hardly competitive with the η except, of course, very close to threshold ($\Delta=m_\eta=549$ MeV). Applying Eq. (26) to the transition $\psi'(2S)\to\psi(1S)$, the only case where data are available, we obtain $r=0.017$, which is in reasonable agreement with the experimental value[3] $r_{\rm expt}=0.037\pm0.0092$.

We shall analyze the predictions of our model in terms of two sets, displayed in columns A and B of Tables I and II, to which we refer as unnormalized and renormalized sets. Set A corresponds to the primitive version with $\alpha_s^E=\alpha_s^M=1$. The results in set B are applied two corrections: (i) $\alpha_s^E=1.12,\alpha_s^M=18$; (ii) physical threshold value $W_{\rm min}=2m_\pi$. For the 0^- channel cases where only π^0 emission is energetically allowed (recognizable by the condition $\Delta\le m_\eta$) we apply further the correction in Eq. (26), setting $x=1$, of course.

The variation of the integrated rates with quark mass is displayed in Fig. 5, in anticipation of future toponium studies. One observes an initial fast fall off of the mass dependence followed by a slower one but no leveling. The general behavior seen here is easily explained as a result of the compensation between the decrease of the

TABLE II. Hadronic transition rates Γ in keV in the $b\bar{b}$ system. For each initial- and final-state configuration, the first line gives the $0^+=\pi^+\pi^-\oplus\pi^0\pi^0$ rates and the second line the $0^-=\eta\oplus\pi^0$ rates. The predictions found in this work are presented in an unrenormalized version (column A) ($\alpha_s^E=1$, $\alpha_s^M=1$) and in a renormalized version (column B) enclosed inside brackets which incorporates three corrections: (1) hadronization probability $\alpha_s^E=1.12$, $\alpha_s^M=18$; (2) phase space with threshold value $W=2m_\pi$; (3) the extra factor in Eq. (26) for π^0 emission. The VZSN (Refs. 9–12) predictions refer to the low-energy approach. The Kuang-Yan[13,14] model predictions labled by KY1 refer to the vibrating string model and those labeled by KY2, enclosed inside brackets, refer to the partonic two-gluon model. The experimental data are extracted from Ref. 2 and from the compilation Ref. 21.

Transition	Δ (MeV)	This work A	B	VZSN	Multipole KY1	[KY2]	Expt.
$\Upsilon'(2S)\to\Upsilon(1S)+0^\pm$	560	9.8 3.8×10^{-3}	[12.0] [0.64×10^{-1}]	 3.6×10^{-2}	7 1×10^{-2}	[6] [3×10^{-2}]	12 ± 2.5
$\Upsilon''(3D)\to\Upsilon(1S)+0^\pm$	892	3.62 1.7×10^{-3}	[4.6] [0.33×10^{-1}]	16.5 0.16	0.3 3×10^{-3}	[0.2] [0.4]	1.29 ± 0.35
$\Upsilon''(3S)\to\Upsilon'(2S)+0^\pm$	332(pi^0)	2.06 0.31×10^{-3}	[1.25] [0.1×10^{-5}]	0.76	0.6	[4] [3×10^{-2}]	1.01 ± 0.49
$\Upsilon'''(4S)\to\Upsilon(1S)+0^\pm$	1170	0.79 0.21×10^{-3}	[0.98] [0.42×10^{-2}]				
$1^3D_J\to\Upsilon(1S)+0^\pm$	697	18.2 18.1	[14.2] [14.1]	0.105 0.105	24		
$2p_J\to1P_J+0^+$	364	1.66	[1.41]		0.4	[0.3–0.4]	
$1^1P_1-\Upsilon(1S)+0^\pm$	429 (π^0)	0.84 0.85	[2.82] [0.31×10^{-2}]				
$1^3P_1\to\eta_b(1S)+0^+$	429	0.85×10^{-1}	[0.88]				
$1^3P_{J=\binom{0}{2}}\to\eta_b(1S)+0^-(\pi^0)$		0.28 0.88	[0.33×10^{-2}] [0.21×10^{-2}]				
$2^3P_1\to\eta_b(1S)+0^+$	793	0.11	[2.0]			[0.6]	
$2^3P_{J=\binom{0}{2}}\to\eta_b(1S)+0^-$		0.33 0.95	[6.17] [10.1]	0.3			
$\Upsilon''(3S)\to1^1P_1+0^\pm$	463 (π^0)	0.27×10^{-1} 0.27×10^{-1}	[0.13] [0.13×10^{-3}]	1×10^{-3} 2×10^{-2}		[0.2]	$\le0.144\pm0.067$
$\Upsilon'''(4S)\to1^1P_1+0^\pm$	688	0.304×10^{-1} 0.308×10^{-1}	[0.30] [0.31]				

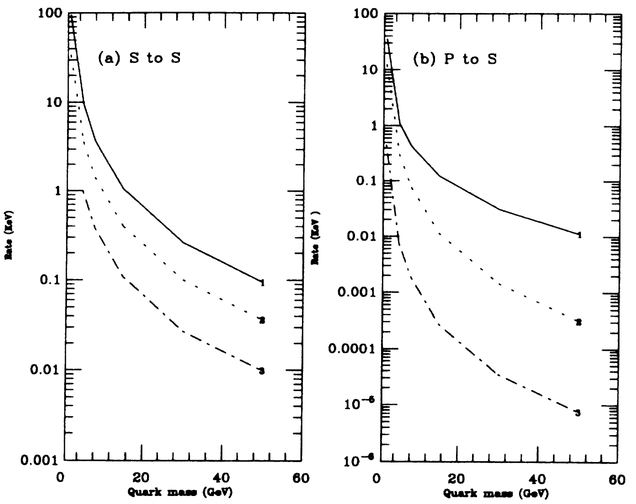

FIG. 5. Dependence on quark mass of integrated rates. (a) refers to the three 0^+ transitions $2S \rightarrow 1S, 3S \rightarrow 1S, 3S \rightarrow 2S$ designated by the labels 1,2,3 and (b) refers to the 0^+ transitions $2P \rightarrow 1P$, $2\,^3P \rightarrow 1\,^1S$, $3\,^3S \rightarrow 1\,^1P$ designated by the labels 1,2,3.

operator and the simultaneous shrinkage of the wave functions. By contrast, in the multipole approach,[13] one found an early leveling off of the rates which sets in at quark masses $m \simeq 15$ GeV.

V. DISCUSSION OF RESULTS AND CONCLUSIONS

We have pursued in this work the semiperturbative Feynman-graph approach initiated by BLMN (Ref. 5) and have applied it in a systematic way to existing as well as prospective data.

The main basis for the $j=0$ projection on the two-gluon intrinsic states is (1) the experimentally verified fact that the angular distributions in the relative $\pi\pi$ angle are essentially isotropic and (2) the anticipated dominance at low energies of the low partial waves, especially the scalar channel, in the $\pi\pi$ system. The latter property is motivated by the π-π phase shifts data and by the fact that the tensor mesons become important at masses significantly higher than 1 GeV. The vector mesons are not relevant since the allowed state of two real (massless) gluons, as also the allowed charge-conjugation-even states of two pions, are $j^{PC}=0^{\pm +}, 2^{\pm +}, \ldots$.

As was first observed by BLMN (Ref. 5), the projection $j=0$ is crucial to reproduce the observed suppression at low W. (At the large W end, the $j=0$ wave saturates exactly the total summed rate.) The suppressed spectrum at small W is a characteristic property of the SS transitions. This property need not hold for the DS and PS transitions, as shown by our results. Let us note however that the peak we obtain at low W for the DS transition does not show up in the corresponding results of Ref. 15. They also predict drastically suppressed DS rates, whereas our predicted rates are comparable to the total unprojected rates and hence large. The origin of the disagreement seems to lie in the prescription used in Ref. 5 to retain only the diagonal matrix elements with respect to the angular momentum projections of the heavy-quark states, which then results in suppressing the orbital momentum L between the heavy-quark system and the two-gluon system. The off-diagonal ($L=2$) matrix elements are responsible for the enhancement at the low W end which is found in our predictions. In the PS transitions too, the off-diagonal ($L=1$) contributions are responsible for the peaking at low W.

In contrast with our findings, an important suppression of the DS and PS transitions is found to take place in the local approximation version of the multipole expansion approach. The suppression is not due to a restriction on the angular momentum of the gluon pair. It arises there mainly because of the absence for the DS and PS transition amplitudes, as opposed to the SS amplitudes, of the trace anomaly contribution.[11,12] On the other hand, the nonlocal models considered by Kuang and Yan,[13] to the extent that they are not subject to the local approximation, yield predictions which are roughly consistent with ours.

Whereas the angular momentum projection prescription is reasonably well motivated, the assumption that the probabilities for the conversion of gluons into hadrons are to be set uniformly to unity, is certainly untenable in view of our results. We have seen that a relative factor of order 20 to 50 is needed in passing from the 0^+ to the 0^- channels in order to match the model with the observations. We expect large uncertainties in this factor coming from the phase-space-correction effects and from the various other technical approximations invoked in obtaining the formulas in Eqs. (14)–(17). Whether this factor reflects an anomalous color-magnetic moment of the heavy quarks or is due to a nonperturbative enhancement effect which, by reference to the prediction of VZNS, reflects the axial-vector-current anomaly, is difficult to decide. It is in any case reassuring to note that our adjusted ratio $\alpha_s^M/\alpha_s^E=(1+\kappa)^2 \simeq 16$ is consistent with independent estimates reached in Ref. 23 for the anomalous color-magnetic moment $\kappa \simeq 1-2$.

The characteristic shapes of our spectra for the SS and DS transitions (Figs. 2 and 4) suggest as an attractive explanation of the flat spectrum observed in the $\Upsilon(3S) \rightarrow \Upsilon(1S)+\pi\pi$ transition the possibility of a D-state admixture. Let us consider for the Υ'' wave function the combination $3\,^3S_1+\epsilon_D 1\,^3D_1$. By applying our formalism to this mixed state we find that the transition rate is given by the incoherent sum $(SS)^2+\epsilon_D^2(DS)^2+2\epsilon_D(SS)(DS)$. In the last interference term, the product of (DS) and (SS) matrix element receives a contribution from the diagonal terms in the angular momentum projections only, so similarly to the $(SS)^2$ term, this term vanishes at small W and is peaked at large W. The only remaining possibility to raise the spectrum at low W rests on the $\epsilon_D^2(DS)^2$ term, whose peaking at low W arises, as noted already, from the off-diagonal terms.

By a simple inspection of Fig. 4(b), we may see that the adjusted value for the D-state probability amplitude needed to fit the data is approximately $\epsilon_D \simeq 0.3$. The typical estimates [23,24] appropriate to charmonium give $\epsilon_D \simeq -0.03$ and one expects a smaller mixing in bottomonium since the gluon-exchange tensor force scales as $1/m^2$. Our adjusted value of ϵ_D is considerably larger than the existing estimates, and if taken seriously, would eventually favor the presence of a long-range confining tensor interaction. Although the way of extracting here ϵ_D depends on a ratio of matrix elements, our simple-minded choice of harmonic-oscillator interquark potential may be responsible for large errors. If one could reduce (enhance) the *SS* (*DS*) transition amplitudes, each, say, by a factor of 3, this would bring ϵ_D down by an order of magnitude. Such large modifications appear unlikely, unless the proximity of the open channels $B\bar{B},B^*\bar{B}$ could strongly affect the structure of Υ''. A careful calculation using realistic wave functions would be welcome in order to support or refute our claim that the observed flat spectrum reflects *D*-state admixture.

In conclusion, four main findings obtained in our work deserve special mention. First, we have strengthened the conclusions reached by BLMN (Ref. 5) and confirmed the attractiveness of the gluon emission model in reproducing the data to within a factor 2. Our *DS* transition rates are considerably larger than those found in Ref. 5, because we allow for a finite orbital angular momentum between the gluons and the heavy quarks. Nearly equal widths obtain then for the *DS* transitions in the $\pi\pi$ and η channels.

We have found that the η and single π meson production are strongly suppressed in the *SS* transitions owing to the cancellation of off-shell effects at the initial step corresponding to the emission of gluons. To be consistent with the observed large branching ratio relative to the $\pi\pi$ mode one needs a strong enhancement factor for the 0^- amplitude. This could arise either via an anomalous quark color-magnetic moment at the initial gluon emission step or, at the second hadronization step, via the axial-vector-current anomaly. In fact, the implications just mentioned were already suggested in the multipole expansion approach as a way to explain the mismatch between the predictions of the soft-pion and partonic models. Nevertheless, it is useful to have this point confirmed here on a completely independent basis. If the first interpretation is appropriate and we are justified in allowing a large ratio for $\alpha_s^M/\alpha_s^E \simeq 16$, then not only are the 0^- channels in *SS* and *DS* transitions enhanced but so also are enhanced both the $0^+,0^-$ channels in *PS* transitions. We see some justification here in that our predicted rate for $3\,^3S_1 \to 1\,^1P_1 + \pi\pi$ is remarkably close to the observed rate which is, however, for the moment an upper bound.[2,3] The multipole soft-pion prediction[11] here lies 2 orders of magnitude below. On the other hand, our π^0 emission rate is strongly reduced in comparison to the $\pi\pi$ rate, by contrast to Ref. 11.

Another important information brought out in this work concerns the new predictions for the *PS* and *DS* transitions which our approach supplies without the need of parameter readjustment. Our predictions are consistent with those of Kuang and Yan,[13] especially their partonic model. This is important because in spite of the obvious similarities between our model and theirs, our formulation avoids the long-wavelength and static approximations and treats perhaps more carefully the relativistic spin effects. Finally, we have shown that the $\pi\pi$ spectra for *DS* and *PS* transitions are enhanced at low W due to contributions associated with finite orbital momentum of the pion pair relative to the heavy-quark system. This property has suggested a possible explanation for the flattened $\pi\pi$ spectrum in the $\Upsilon'' \to \Upsilon$ transition in terms of a *D*-state admixture in the Υ''. However, the needed admixture probability comes out an order of magnitude too large. To established this claim on firm grounds it appears necessary to pursue the calculations using realistic inputs.

ACKNOWLEDGMENTS

Thanks are due to Dr. A. Billoire, Dr. H. Cornille, Dr. R. Lacaze, and Dr. P. Moussa for discussions and to C. Verneyre for help in computing. Service de Physique Théorique is Laboratoire de l'Institut de Rechereche Fondamentale du Commissariat à l'Energie Atomique.

[1]G. Abrams *et al.*, Phys. Rev. Lett. **34**, 1181 (1975).
[2]T. Bowcock *et al.*, Phys. Rev. Lett. **58**, 307 (1987); I. C. Brock, in *Hadrons, Quarks and Gluons*, proceedings of the 22nd Rencontre de Moriond, Les Arcs, France, 1987, edited by J. Tran Than Van (Editions Frontières, Gif-sur-Yvette, France, 1987).
[3]L. S. Brown and R. Cahn, Phys. Rev. Lett. **35**, 1 (1975); M. Voloshin, Pis'ma Zh. Eksp. Teor. Fiz. **21**, 733 (1975) [JETP Lett. **21**, 347 (1975)]; R. Cahn, Phys. Rev. D **12**, 3559 (1975).
[4]H. Goldberg, Phys. Rev. Lett. **35**, 605 (1975).
[5]A. Billoire, R. Lacaze, A. Morel, and H. Navelet, Nucl. Phys. **B155**, 493 (1979).
[6]K. Gottfried, Phys. Rev. Lett. **40**, 598 (1978); M. B. Voloshin, Nucl. Phys. **B154**, 365 (1979).
[7]M. E. Peskin, in *Dynamics and Spectroscopy at High Energy*, proceedings of the Eleventh SLAC Summer Institute on Particle Physics, Stanford, California, 1983, edited by P. M. McDonough (SLAC, Report No. 267, Stanford, 1984).
[8]T. M. Yan, Phys. Rev. D **22**, 1652 (1980).
[9]M. B. Voloshin and V. Zakharov, Phys. Rev. Lett. **45**, 688 (1980).
[10]V. A. Novikov and M. A. Shifman, Z. Phys. C **8**, 43 (1981).
[11]M. B. Voloshin, Yad. Fiz. **43**, 1571 (1986) [Sov. J. Nucl. Phys. **43**, 1011 (1986)].
[12]P. Moxhay, Phys. Rev. D **37**, 2557 (1988).
[13]Y. P. Kuang and T. M. Yan, Phys. Rev. D **24**, 2874 (1981).
[14]Y. P. Kuang, S. F. Tuan, and T. M. Yan, in *Hadron 1987*, proceedings of the 2nd International Conference on hadron Spectroscopy, Tsukuba, Japan 1987, edited by Y. Oyanagi, K. Takamatsu, and T. Tsuru (KEK Report No. 87-7, Tsukuba, 1987); Phys. Rev. D **37**, 1210 (1988).
[15]G. Belanger, T. DeGrand, and P. Moxhay, Phys. Rev. D **39**, 257 (1989); M. B. Voloshin, Pis'ma Zh. Eksp. Teor. Fiz. **37**, 58 (1983) [JETP Lett. **37**, 69 (1983)].
[16]H. J. Lipkin and S. F. Tuan, Phys. Lett. B **206**, 349 (1988); Phys. Rev. Lett. **62**, 2910 (1989).
[17]R. Blankenbecler and L. F. Cook, Jr., Phys. Rev. **119**, 1745 (1960); R. G. Arnold, C. E. Carlson, and F. Gross, Phys. Rev.

C **21**, 1426 (1980).
[18]R. Blankenbecler and R. Sugar, Phys. Rev. **142**, 1051 (1966).
[19]R. Barbieri and E. Remiddi, Nucl. Phys. **B141**, 413 (1978).
[20]G. C. Wick, Ann. Phys. (N.Y.) **18**, 65 (1962); M. I. Shirokov, Zh. Eksp. Teor. Fiz. **40**, 1387 (1961) [Sov. Phys. JETP **13**, 975 (1961)].
[21]Particle Data Group, G. P. Yost *et al.*, Phys. Lett. B **204**, 1 (1988).
[22]D. Gross, S. Treiman, and F. Wilczek, Phys. Rev. D **19**, 2188 (1979).
[23]V. A. Novikov, L. B. Okun, M. A. Shifman, A. I. Vainshtein, M. B. Voloshin, and V. I. Zakharov, Phys. Rep. **41**, 1 (1978).
[24]E. Eichten, K. Gottfried, T. Kinoshita, K. Lane, and T. M. Yan, Phys. Rev. D **21**, 203 (1980).